CHEMISTRY

Pd(II)-catalyzed carboxylation of aromatic C—H bonds with CO_2

Gregor Kemper[1], Markus Hölscher[1]*, Walter Leitner[1,2]*

The carboxylation of nonactivated C—H bonds provides an attractive yet hitherto largely elusive chemical process to synthesize carboxylic acids by incorporation of CO_2 into the chemical value chain. Here, we report on the realization of such a reaction using simple and nonactivated arenes as starting materials. A computationally designed Pd(II) complex acts as organometallic single-component catalyst, and apart from a base, necessary for thermodynamic stabilization of the intermediates, no other additives or coreagents are required. Turnover numbers up to 10^2 and high regioselectivities are achieved. The potential of this catalytic reaction for "green chemistry" is demonstrated by the synthesis of veratric acid, an intermediate for pharmaceutical production, from CO_2 and veratrol.

INTRODUCTION

The utilization of carbon dioxide (CO_2) is expected to play a key role on the way to a circular and sustainable production of chemical goods (*1*–*6*). Among the many interesting transformations of CO_2, the carboxylation of C—H bonds to obtain carboxylic acids is equally attractive and challenging (*7*–*13*). In particular, the catalytic carboxylation of nonactivated C—H bonds in arenes would open a potential "green chemistry" route to aromatic carboxylic acids, which are frequent motives in high-value chemicals and biologically active products. On the way to realize these dream reactions, several important steps have already been taken, but major challenges in terms of sustainability and applicability still remain unsolved.

The uncatalyzed carboxylation of certain phenolate salts as activated substrates, known as the Kolbe-Schmitt reaction, is used in industry for a long time in the production of salicylic acid (*14*). Catalytic coupling reactions of preactivated arenes, such as organo-zinc (*15*) or organo-boron (*16*–*18*) compounds or aryl (pseudo)-halides (*19*–*23*) with CO_2, have also been studied in detail, with preactivation also being conducted in situ (*24*). The catalytic insertion of CO_2 into C—H bonds of aromatic substrates is comparably very rare, however, and hitherto restricted mainly to C—H acidic [pK_a (where K_a is the acid dissociation constant) < 30.3] and hence very electron-deficient aromatics as reported, for example, by the groups of Nolan and Hou (Fig. 1A, top) (*25*–*27*). Similarly, inter alia, the groups of Ackermann, Hu, and Kanan showed carboxylation of C—H acidic heteroarenes with CO_2 under transition metal-free conditions using KO^{t}Bu or carbonates for deprotonation (*28*–*31*). The group of Iwasawa was able to convert simple arenes, like benzene, directly to carboxylic acids using a Rh catalyst (Fig. 1A, middle) (*32*–*34*). However, their protocol requires the utilization of stoichiometric amounts of expensive, energy intensive, and pyrophoric alkyl aluminum coreagents, and the chemoselectivity and regioselectivity of the reaction remained limited for substituted arenes. The groups of Yu and Li combined aromatic C—H carboxylation with intramolecular cyclization to yield lactones or lactams (Fig. 1A, bottom) (*35*–*38*). Although no stoichiometric amounts of organometallic additives are needed in these reactions, they are applicable only to a specific class of substrates and yield acid derivatives as products. Other attempts to achieve the transformation include reactions occurring via transition metal migration from reactive directing groups (*39*, *40*) or photocatalytic carboxylation of naphthalenes and heteroarenes (*41*).

Consequently, the development of a catalytic system that directly accesses carboxylic acids from arenes and CO_2 in high selectivity remains a very desirable goal. In particular, electron-rich substituted aromatics as derived from lignin biomass would seem to be attractive starting materials in post-fossil economies. While the presence of a base is mandatory to render this endergonic reaction thermodynamically feasible by passing through the carboxylate salts as intermediates, other coreagents, especially hazardous ones, need to be avoided in accord with the principles of green chemistry. Here, we present the first example of a catalytic system that fulfills these criteria.

Our long-term strategy to develop such a catalytic system was based on a combined approach of computational and experimental chemistry. Inspired by the well-known hydrogenation of CO_2 to formic acid (*7*, *42*, *43*), an analogous catalytic cycle was designed consisting of a carboxylate-assisted C—H bond activation under formation of a reactive metal-carbon bond [concerted metalation deprotonation (CMD) type] (*44*, *45*) and base-assisted liberation of the acid product (Fig. 1C, right-hand side). The well-established insertion of CO_2 into a M—C bond as a key step generates the aryl carboxylate (Fig. 1C, left-hand side) that acts again as a recipient of the formal proton from the C—H bond. Density functional theory (DFT) calculations confirmed the principle feasibility of such a redox-neutral catalytic cycle (*46*, *47*), indicating that the migratory insertion of CO_2 into a metal-aryl bond would be turnover-determining. From a systematic in silico screening, phosphine sulfonamido Pd(II) complexes were identified as lead structures providing sufficiently low energy spans from computation corresponding to the overall experimental activation barrier. The CO_2 insertion into palladium-aryl bonds of these complexes was confirmed as stoichiometric reaction experimentally (*48*). Complex **1** (Fig. 1C, middle) was predicted as a promising catalyst

[1]Institut für Technische und Makromolekulare Chemie, RWTH Aachen University, Aachen, Germany. [2]Max Planck Institute for Chemical Energy Conversion, Mülheim an der Ruhr, Germany.
*Corresponding author. Email: walter.leitner@cec.mpg.de (W.L.); hoelscher@itmc.rwth-aachen.de (M.H.)

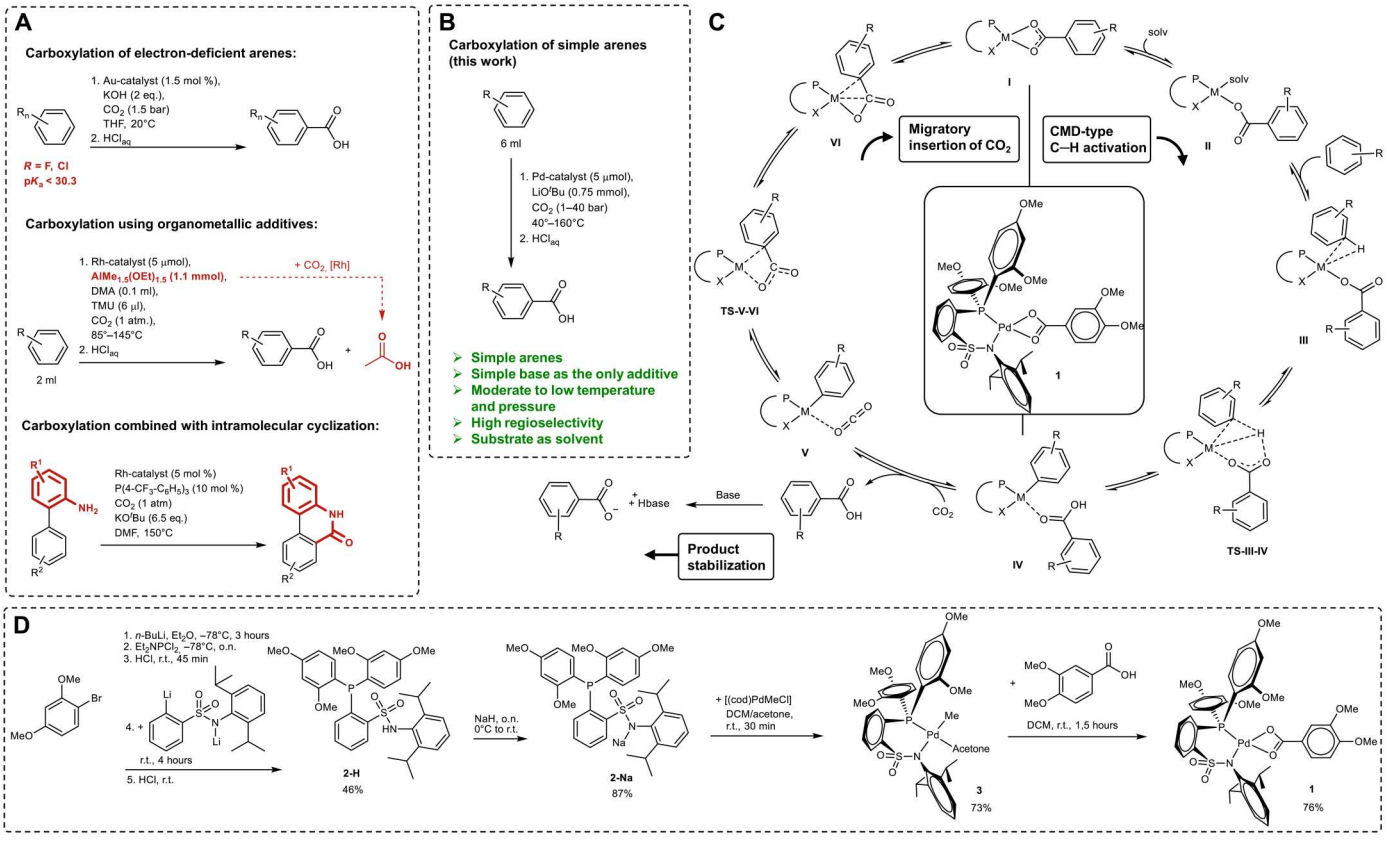

Fig. 1. Catalytic carboxylation of arenes with CO_2. (**A** and **B**) Selected previously (A) and here (B) reported examples of approaches involving the direct catalytic carboxylation of arenes with CO_2 (*26*, *34*, *38*). mol %, mole percent. (**C**) Generalized generic computationally proposed catalytic cycle and catalyst **1** for the direct carboxylation of arenes with CO_2 (*46*, *48*, *49*); TS , transition state. (**D**) Synthesis of Pd(II) catalyst **1** (*48*, *50*, *51*). o.n., overnight; r.t., room temperature.

from a computational variation of all relevant reaction parameters (*49*).

We now report the successful transfer of these fundamental results to the homogeneously catalyzed carboxylation of aromatic C—H bonds with CO_2 and report its application to a number of arenes without the need for preactivation, directing groups, or stoichiometric amounts of organometallic additives (Fig. 1B). Unprecedented synthetic routes to aromatic carboxylic acids are opened with this approach as demonstrated for the combination of bio-based veratrol with CO_2 to yield veratric acid as example of an important pharmaceutical motif.

RESULTS AND DISCUSSION

The synthesis of the computationally designed phosphine sulfonamido Pd(II) complex **1** was achieved, adapting a previously established route for similar complexes (Fig. 1D) (*48*, *50*). Ligand **2-H** is obtained readily on gram scale from the corresponding bromo arene and the substituted sulfonamide in a single reaction sequence without the need for intermediate purification steps (*50*, *51*). After deprotonation, **2-Na** is treated with [(cod)PdMeCl] to yield complex **3** that is further converted by the addition of 3,4-dimethoxybenzoic acid (DMBA) to the desired precatalyst **1**.

To test the catalytic activity of complex **1**, 1,3-dimethoxybenzene (DMB; **4**) was chosen as a substrate for the initial screening because the product can be readily distinguished in the reaction mixture from the isomeric acid 3,4-DMBA (**6**), which is liberated from the carboxylate present in the precatalyst. Turnover numbers (TONs) can thus be determined directly using **6** as the internal standard as verified by addition of 1,3,5-trimethoxybenzene as the external standard after the workup (see the Supplementary Materials for details). We note that the substrate must be completely free of phenolic impurities to avoid undesired Kolbe-Schmitt carboxylation as a side reaction.

An initial screening showed that product formation could be achieved in neat substrate, while classical organic solvents showed limited compatibility with the catalyst due to poor solubility (e.g., alkanes), decomposition at elevated temperatures [dichloromethane (DCM) and $CHCl_3$], or possibly strong coordination [e.g., tetrahydrofuran (THF) and dimethyl sulfoxide]. In the standard procedure, complex **1** was dissolved in 1,3-DMB and a suspension with KO^{t}Bu (150 eq.) was pressurized with CO_2 (40 bar) in a stainless-steel high-pressure reactor. After a reaction time of 19.5 hours at 100°C and subsequent acidic workup, 2,4-DMBA (**5a**, 44 eq.) was isolated (Fig. 2A, entry 1). The identity of the product was confirmed by nuclear magnetic resonance (NMR) spectroscopy, high-resolution mass spectrometry (HRMS), and x-ray diffraction analysis (see the Supplementary Materials). Incorporation of the CO_2 molecule as the C1 source for the carboxylate group was confirmed using isotopically labeled $^{13}CO_2$, resulting in a 100×

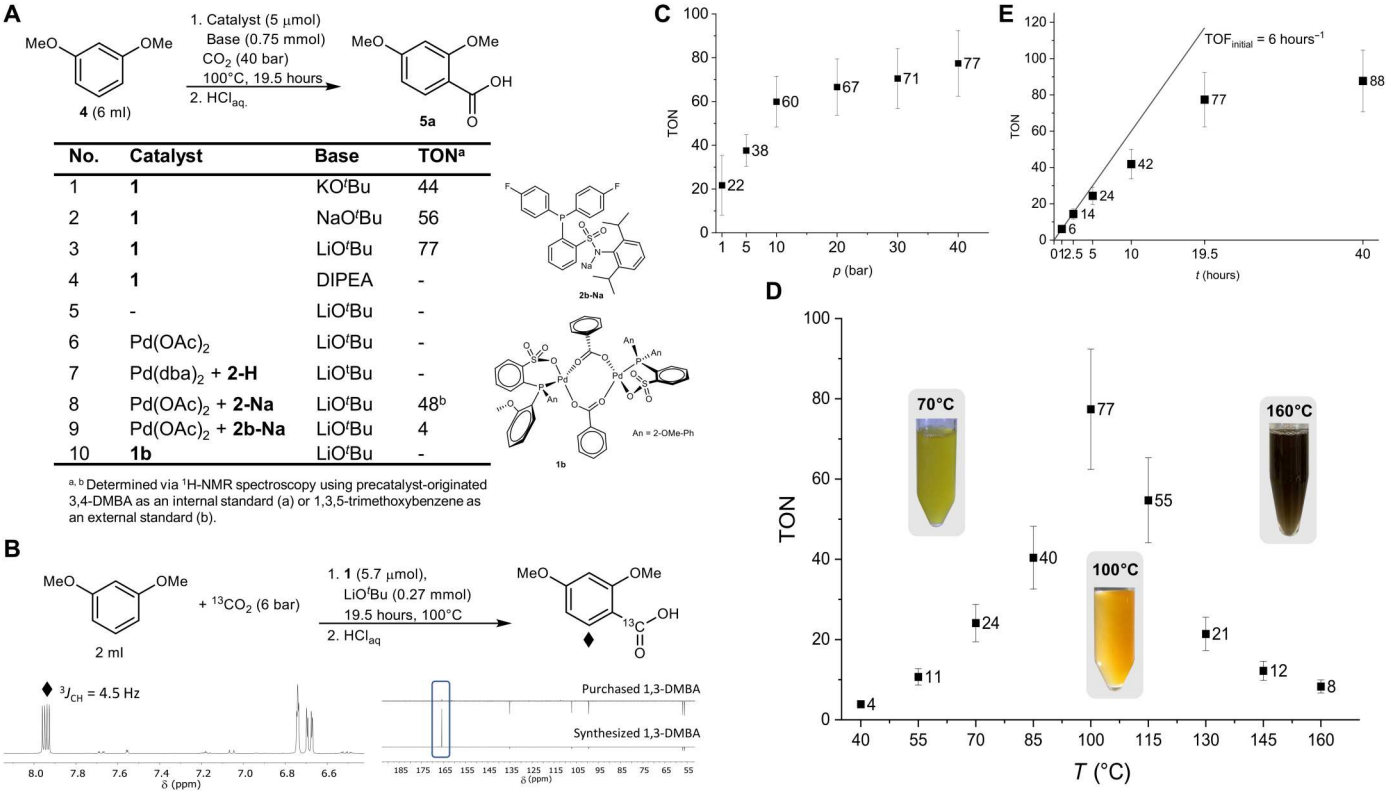

No.	Catalyst	Base	TON[a]
1	**1**	KO^{t}Bu	44
2	**1**	NaO^{t}Bu	56
3	**1**	LiO^{t}Bu	77
4	**1**	DIPEA	-
5	-	LiO^{t}Bu	-
6	$Pd(OAc)_2$	LiO^{t}Bu	-
7	$Pd(dba)_2$ + **2-H**	LiO^{t}Bu	-
8	$Pd(OAc)_2$ + **2-Na**	LiO^{t}Bu	48[b]
9	$Pd(OAc)_2$ + **2b-Na**	LiO^{t}Bu	4
10	**1b**	LiO^{t}Bu	-

[a, b] Determined via ^{1}H-NMR spectroscopy using precatalyst-originated 3,4-DMBA as an internal standard (a) or 1,3,5-trimethoxybenzene as an external standard (b).

Fig. 2. Variation of reaction parameters. (**A**) Initial catalytic carboxylations of 1,3-DMB with catalyst **1** and catalyst variation. (**B**) Carboxylation of 1,3-DMB using ^{13}C-labeled CO_2 (top) and relevant regions of ^{1}H-NMR (bottom left) and ^{13}C-NMR spectra (bottom right) in acetone-d_6. (**C** to **E**) CO_2 pressure (C), temperature (D), and time (E) dependency of productivity for the direct carboxylation of 1,3-DMB with catalyst **1** including photographs of reaction medium after the reaction at 70°, 100°, and 160°C. Reaction conditions as described for (A). Given values represent arithmetic means of at least two independently conducted experiments. Error bars represent the conservative relative 95% confidence interval of ±19%, which was estimated on the basis of all data points (see the Supplementary Materials).

intensified signal in ^{13}C-NMR and a $^3J_{CH}$ = 4.5-Hz coupling in ^{1}H-NMR spectra (Fig. 2B).

In accord with our previous calculations (*49*), *tert*-butoxides were proven as suitable bases, while amines such as Hünig's base [diisopropylethylamine (DIPEA)] were not effective (Fig. 2A, entries 2 to 4). Because of its good solubility in organic reaction medium, LiO^{t}Bu was chosen for further systematic studies, while the cheaper potassium or sodium salts may be used preferentially for practical reasons. In the absence of complex **1**, no reaction was observed (entry 5). Similarly, $Pd(OAc)_2$ in the absence of ligand (entry 6) or $Pd(dba)_2$ as a Pd(0) source in combination with the protonated ligand **2-H** (entry 7) was also proven inactive. The latter result is in line with the redox-neutral reaction mechanism used as basis for the computational design rather than an alternative oxidative addition/reductive elimination pathway. The active catalyst can be formed also in situ by applying $Pd(OAc)_2$ as a precatalyst in combination with ligand **2-Na** (entry 8), albeit at slightly reduced TONs as compared to reactions using complex **1**.

To validate further the computational design, two structurally related ligands were evaluated for which the calculations predicted lower or even no activity (*49*). The less electron-rich phosphine sulfonamido ligand **2b** gave only a TON of 4 in line with the substantially higher energy span determined for the presumed mechanism (entry 9). For phosphine sulfonato ligands, the calculations revealed a thermodynamic driving force to form preferentially dimeric carboxylato complexes rather than the active monomeric complexes (**I**), thus acting as deactivated off-loop species. The dimeric structure was verified experimentally via x-ray diffraction analysis of complex **1b** (see the Supplementary Materials) that proved to be catalytically inactive as predicted (entry 10).

To evaluate the influence of reaction conditions on the performance of the successful catalyst **1**, the temperature and CO_2 pressure were varied systematically. In a CO_2 pressure range between 20 and 45 bar, no significant dependency in productivity is observed (Fig. 2C and table S1). However, the TON decreases upon further lowering the pressure, indicating that the elementary step of CO_2 insertion becomes involved in turnover limitation as predicted computationally. Nevertheless, even at a pressure as low as 1 bar, considerable turnover can be detected. In all catalytic reactions presented in this work, the reaction vessels were pressurized for a period of 20 min at room temperature before starting the reaction. Shorter pressurizing times resulted in a decrease in pressure during the starting time due to further dissolution of CO_2 and formation of hemicarbonate (LiOOCO^{t}Bu). It cannot be excluded that this salt is also involved in the C—H activation step as recently reported by the group of Fu for the synthesis of aryl lactones (*52*). Because of pressure variations in the CO_2 supply during the pressuring time spans, the starting pressure in the following experiments varied by approximately ±5 bar. However, this does not affect the productivity at the applied pressures, as mentioned above.

Variation of the reaction temperature results in a nearly exponential increase in TON at temperatures up to 100°C as expected under kinetic limitations (Fig. 2D and table S1). Further increase in temperature results in a strong decrease in productivity, very likely induced by faster catalyst decomposition at these temperatures. The color of the reaction medium after the reaction changes from slight yellow over bright orange to black at high temperatures (Fig. 2D) in line with our previous observations of orange-colored dimeric complexes as a primary decomposition product in similar reactions (*48*). The conversion/time profile of the reaction at 100°C (Fig. 2E and table S1) reveals an initial turnover frequency (TOF) of 6 hours^{-1}, which decreases at prolonged reaction time, leveling out a productivity of TON = 88 after 40 hours when the observed color change indicated catalyst decomposition. At lower temperatures, however, productivity continues to increase when prolonging the reaction time, resulting in a TON of 103 after 670 hours at 55°C. The activation energy estimated from a set of time/yield reactions at low temperatures (see the Supplementary Materials) amounts to 25 kcal mol^{-1} in good agreement with the energy spans δE derived from previous calculations with the predicted catalyst (26.8 kcal/mol for carboxylation of 1,2-DMB, vide infra) (*49*).

Upon carboxylation of 1,3-DMB as a substrate, the formation of three isomers—2,4-DMBA, 3,5-DMBA, and 2,6-DMBA—is possible in principle. However, at reaction temperatures of up to 130°C, 2,4-DMBA (**5a** in Fig. 3A) is formed with a remarkable selectivity of more than 95%. Again, the preferred formation of this isomer is in accordance with the redox-neutral mechanism for which the computational analysis shows lower energy barriers for CO_2 insertion at more electron-rich carbon atoms (*46*, *49*). The formation of 2,6-DMBA (**5c**) having two electronically donating *ortho*-OMe groups is nearly completely suppressed under all conditions applied (<1%) due to steric shielding of the reactive carbon atom. *Bis-ortho*-methoxy–substituted benzoic acids undergo fast protodecarboxylation catalyzed by a similar Pd-complex (*48*). At temperatures ≥130°C, additional formation of 2-hydroxy-4-methoxybenzoic acid (**7**) and trace amounts of 2-hydroxy-4-methoxyisophthalic acid are observed. These products very likely originate from selective mono-dealkylation of 1,3-DMB as described by the group of Loh (*53*), followed by noncatalytic Kolbe-Schmitt reaction.

The discovered catalytic method was applied to a range of aromatic substrates comprising nonactivated C—H bonds (Fig. 3B). For 1,2-DMB (**8**) and anisole (**9**), the reaction proceeded smoothly with slightly lower TONs as compared to 1,3-DMB. The reaction of 1,2-DMB almost exclusively forms 3,4-DMBA (>99%), confirming the effect of steric hindrance and excluding the possibility that the methoxy substituents would act as ortho-directing groups as reported for the Iwasawa system (*31*–*33*). Anisole shows similar but slightly less pronounced regioselectivity due to higher similarity of the potentially reactive carbon atoms regarding their electron density and their steric accessibility. In line with this argument, the carboxylation of 1-methoxynaphthalene (**11**) and 1,3-benzodioxole (**13**)—which offer several potentially reactive positions—also occur with pronounced regioselectivity in the most electron-rich and sterically least hindered positions. The trend is also reflected in the relative reactivities of toluene (**15**) and benzene (**17**) (entries 6 to 8). It was ascertained that the conversion of benzene to benzoic acid under standard conditions is a metal-catalyzed reaction (entries 7 and 8), demonstrating the principle feasibility even for this extremely challenging transformation. Halide substituents are tolerated also, and carboxylation at the C-X position occurs only as a minor side reaction as seen with bromobenzene (**19**) and bromoanisole (**21**). Amine-functionalized aromatics can also be applied as shown by catalytic carboxylation of *N*,*N*-dimethyl aniline (**23**) to dimethylated *para*-aminobenzoic acid (also known as vitamin B_{10}). The generally observed increasing productivity at carbon atoms, having enhanced electron density, strongly supports our previous computational considerations (*49*). On a mechanistic level, this can either be explained by facilitated electrophilic C—H activation following the predicted CMD mechanism or by faster CO_2 insertion into the more electron-rich Pd—C bonds (*46*). Because of the variety of electron-rich compounds that can be found in renewable feedstocks, such as lignin-derived methoxy-substituted derivatives, this method complements well the former progress in this field (*25*–*31*), which relies on different C—H activation mechanisms and is therefore restricted to electron-deficient heteroarenes on a practical scale.

To explore the synthetic applicability of the reaction, a gram-scale carboxylation of veratrole (1,2-DMB, **8**) was conducted (Fig. 4). This substrate was chosen because it can easily be produced from guaiacol (*54*), one of lignin′s main depolymerization products (*55*). The obtained product veratric acid (**6**) represents an important feedstock for pharmaceutical industry, for example, in the synthesis of the gastrointestinal drug itopride (*56*) and has antioxidant and anti-inflammatory activities itself (*57*, *58*). The experiment was conducted using the in situ catalyst formed from $Pd(OAc)_2$ with ligand **2-Na**, avoiding the organometallic step for catalyst preparation. Under relatively mild conditions [T = 85°C, $p(CO_2)$ = 13 bar, t = 44 hours], the reaction proceeded smoothly to reach 70% yield based on the base as limiting component (TON =), and 1.76 g of veratric acid was obtained after standard workup in high purity according to NMR spectroscopic analysis. These results agree well with experiments conducted under the same conditions in small scale (Fig. 3B, entry 2 and the Supplementary Materials), indicating the potential for practical scale-up of the reaction even at this early stage of development.

The catalytic carboxylation of nonactivated C—H bonds in aromatic substrates had remained largely elusive in the field of CO_2 utilization so far. The present work achieves this transformation with a molecular Pd(II) catalyst opening novel pathways for the synthesis of aromatic carboxylic acids from readily available starting materials and CO_2. The substrate scope at this early stage comprises simple arenes such as benzene and toluene and substituted aromatic compounds bearing alkoxy, amino, and, to some extent, also halide functionalities. This includes aromatic structures as derived from lignin opening fully defossilized "biohybrid" (*59*) reaction paths to aromatic carboxylic acids as encountered in biologically active products and pharmaceuticals.

In addition to the practical potential of this transformation for green chemistry, the successful development of a so far unknown catalytic reaction provides an example for molecular catalyst design from first principles. The catalytic system that proved effective in this work was the result of the systematic computational analysis of a rationally proposed but unprecedented catalytic cycle. Notably, DFT calculations were used ex ante for the design of the catalyst lead structure and for the choice of other components such as the benchmark substrate and the nature of the base. The experimental verification of an unprecedented catalytic reaction

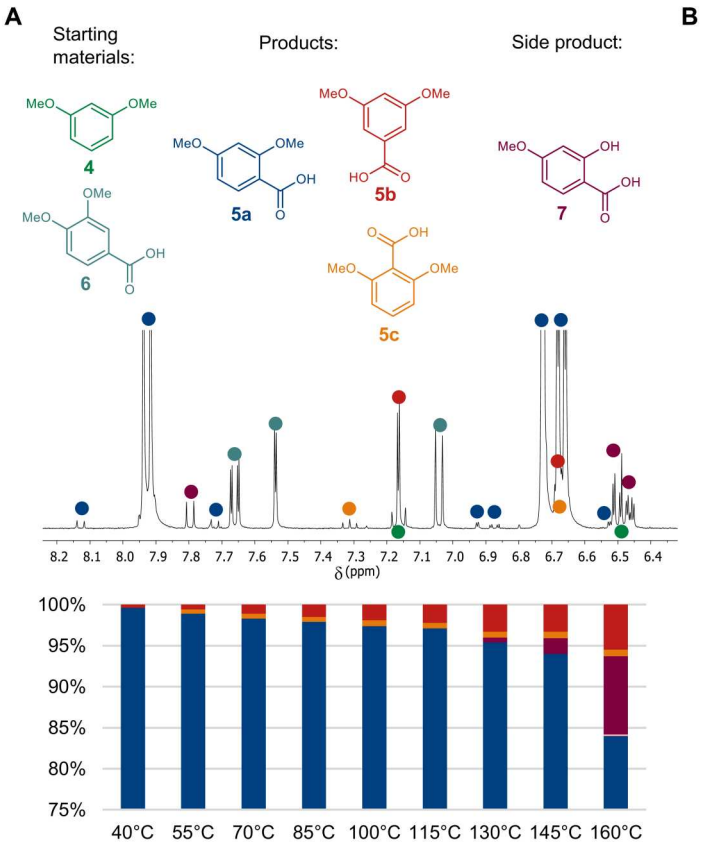

B

No.	Substrate	Main product	Selectivity[a] α:β:γ	TON[b]
1	4	5a	>97:2:<1	77
2	8	6	>99:<1	42[c]
3	9	10	81:8:11	27
4	11	12	62:14:<1:3:7:15:<1 (α:β:γ:δ:ε:ζ:η)	12[c]
5	13	14	76:24	8
6	15	16	63:34:3	4
7	17	18	-	1.5
8[d]	17	-	-	-
9	19	20	94:6:<1:<1	7
10	21	22	62:38:<1	<1
11	23	24	>99:<1:<1	3

[a, b, c] Determined via ^{1}H-NMR spectroscopy using precatalyst-originated 3,4-DMBA as an internal standard (b) or 1,3,5-trimethoxybenzene as an external standard (c). [d] w/o catalyst

Fig. 3. Regioselectivity and substrate scope. (**A**) Observed products of catalytic carboxylation of 1,3-DMB at 145°C and precatalyst originated 3,4-DMBA (top), aromatic region of the ^{1}H-NMR spectrum of this reaction after acidic workup (middle), and shares of different regioisomers and side products yielded at different reaction temperatures (bottom; for tabulated values, see the Supplementary Materials). (**B**) Substrate scope and obtained productivities and regioselectivities. Reaction conditions: substrate (6 ml), **1** (5 μmol), LiO^{t}Bu (0.75 mmol), 19.5 hours, 100°C, and 40-bar CO_2.

demonstrates the increasing potential of computational chemistry to mature from an analytical to a predictive tool in molecular catalysis.

MATERIALS AND METHODS

Materials and general considerations

All manipulations of air- and moisture-sensitive materials were carried out under an atmosphere of argon (Ar) (Argon 4.8 Spectro, Westphalen AG) using standard glove box and Schlenk techniques. Acetone, THF, Et_2O, and DCM were purchased at Acros Organics as extra dry, stored over 4-Å molecular sieves (except for acetone), and degassed by flushing for several hours with Ar. For the extraction of carboxylic acids, a technical grade DCM was used. All methoxy-containing substrates were extracted twice with the same amount of 2 M NaOH and subsequently three times with water. After predrying over Na_2SO_4, the substrates were stored over 4-Å molecular sieves and degassed either by flushing for several hours with Ar (1,3-DMB and 1,2-DMB) or by three consecutive freeze-pump-thaw cycles (all others). Deuterated solvents were supplied by Eurisotop and were degassed by three consecutive freeze-pump-thaw cycles and stored over 4-Å molecular sieves for analysis of air- and moisture-sensitive materials or used as received. All other solvents were purified by redestillation, degassed by bubbling with Ar for several hours, and stored over 4-Å molecular sieves. All other commercially available reagents and starting materials were supplied by Sigma-Aldrich, Acros Organics, or ABCR and used as received. NMR spectra were recorded with a Bruker Ascend 400 spectrometer at 25°C. ^{1}H- and ^{13}C-NMR spectra were referenced to tetramethylsilane; ^{31}P-NMR spectra were referenced to an external 85% H_3PO_4 solution. Coupling constants are given in hertz. X-ray diffraction data were collected at 100 K on a

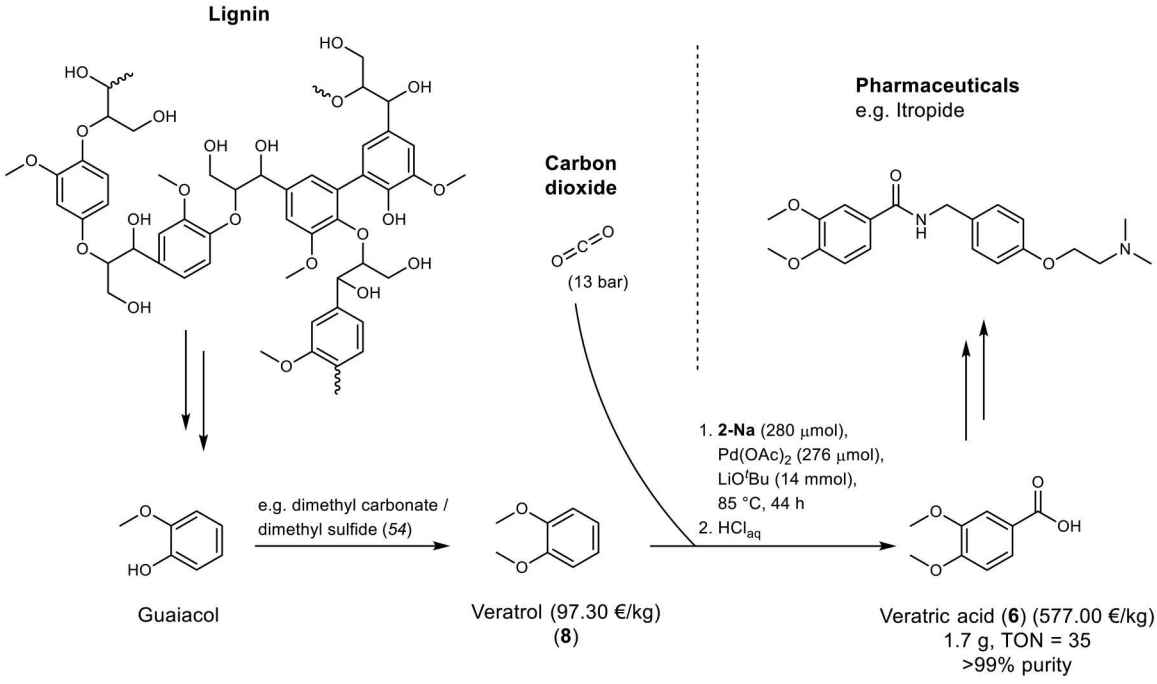

Fig. 4. Gram-scale synthesis of pharmaceutically relevant veratric acid (6) from veratrole (8) and CO_2. Prices from Sigma-Aldrich at the day of submission.

Bruker AXS-Enraf-Nonius Kappa charge-coupled device diffractometer with monochromated Mo Kα radiation (λ = 0.71073 Å). Electrospray mass spectra (ESI-MS) were recorded with a Thermo Scientific Q Exactive Plus or LTQ FT Ultra instrument. Elemental analysis was performed with a PerkinElmer CHNS/O analyzer 2400 instrument.

Synthetic procedures

Synthesis of compound 2-H (48, 50, 51)

A solution of 4654 mg of 1-bromo-2,4-dimethoxybromobenzene (21.44 mmol, 2 eq.) in 40 ml of Et_2O was cooled to −78°C, and 13.4 ml of *n*-BuLi in hexanes (1.6 M, 21.44 mmol, 2 eq.) was added dropwise. After stirring for 3 hours at −78°C, 1838 mg of dichloro(diethylamino)phosphine (10.56 mmol, 0.98 eq.) was added dropwise at −78°C, and the resulting colorless suspension was stirred overnight while warming to room temperature. At 0°C, 10.5 ml of HCl in Et_2O (2 M, 21 mmol, 1.96 eq.) was added dropwise, stirred for 45 min at room temperature, and filtered over Celite (solution **A**). In another flask, 13.4 ml of *n*-BuLi in hexanes (1.6 M, 21.44 mmol, 2 eq.) was added dropwise at 0°C to a solution of 3403 mg of *N*-(2,6-diisopropylphenyl)benzenesulfonamide (10.72 mmol, 1 eq.) in 40 ml of THF and stirred at room temperature for 2 hours, resulting in an orange solution. To this, solution **A** was added at room temperature and stirred for 4 hours and 6 mL HCl in Et_2O (2M, 12 mmol, 1.12 eq) were added. The removal of all volatiles under vacuum resulted in an off-white foam to which 35 ml of EtOH was added at 70°C, which primarily caused all solid to dissolve and subsequently a colorless solid to precipitate. After storing overnight at 3°C, the solid was filtered off at 0°C and washed twice with 5 ml of EtOH. Drying under reduced pressure resulted in 3000 mg of **2-H** (4.83 mmol, 46%) as a colorless solid.

^{1}H-NMR (400 MHz, CD_2Cl_2, 25°C): δ [parts per million (ppm)] = 7.98 (m, 1H, 6-H), 7.50-7.41 (m, 3H, 5-H, 4-H and N-H), 7.29 (t, $^3J_{HH}$ = 7.7 Hz 1H, 16-H), 7.25 (m, 1H, 3-H), 7.17 (d, 2H, $^3J_{HH}$ = 7.7 Hz, 15-H), 6.65 (dd, $^3J_{HH}$ = 8.4 Hz, $^3J_{PH}$ = 5.0 Hz, 2H, 8-H), 6.50 (dd, $^4J_{PH}$ = 4.5 Hz, $^4J_{HH}$ = 2.3 Hz, 2H, 11-H), 6.45 (dd, $^3J_{HH}$ = 8.4 Hz, $^4J_{HH}$ = 2.3 Hz, 2H, 9-H), 3.80 (s, 6H, 20-H), 3.67 (s, 6H, 19-H), 3.30 (hept, $^3J_{HH}$ = 6.8 Hz, 2H, 17-H), and 1.11 (d, $^3J_{HH}$ = 6.8 Hz, 12H, 18-H). ^{13}C{^{1}H}-NMR (101 MHz, CD_2Cl_2, 25°C): δ [ppm] = 162.9 (s, C_q, C10), 162.7 (d, $^2J_{PC}$ = 16.9 Hz, C_q, C12), 149.2 (s, C_q, C14), 147.7 (d, $^2J_{PC}$ = 28.9 Hz, C_q, C1), 136.8 (d, $^2J_{PC}$ = 1.0 Hz, CH, C3), 136.7 (d, $^1J_{PC}$ = 22.7 Hz, C_q, C2), 135.6 (d, $^2J_{PC}$ = 1.5 Hz, CH, C8), 132.2 (s, CH, C4), 131.2 (d, $^5J_{PC}$ = 1.8 Hz, C_q, C13), 129.3 (s, CH, C5), 128.9 (s, CH, C16), 127.4 (d, $^3J_{PC}$ = 5.2 Hz, CH, C6), 124.3 (s, CH, C15), 115.6 (d, $^1J_{PC}$ = 5.4 Hz, C_q C7), 106.0 (d, $^3J_{PC}$ = 1.4 Hz, CH, C9), 99.0 (d, $^3J_{PC}$ = 2.3 Hz, CH, C11), 56.4 (d, $^4J_{PC}$ = 0.7 Hz, CH_3, C19), 55.9 (s, CH_3, C20), 29.2 (s, CH, C17), and 24.4 (s, CH_3, C18). ^{31}P{^{1}H}-NMR (162 MHz, CD_2Cl_2, 25°C): δ [ppm] = −33.71. ESI-MS(pos) [mass/charge ratio (*m*/*z*)]: for $[M + H]^+ = [C_{34}H_{41}NO_6PS]^+$; found (calcd.): 622.23854 (622.23867). Anal. calcd. for $C_{34}H_{40}NO_6PS$: C, 65.68; H, 6.49; N, 2.25; S, 5.16; found: C, 64.32; H, 5.77; N, 2.09; S, 5.33.

Synthesis of ligand 2-Na

One thousand five hundred milligrams of compound **2-H** (2.41 mmol, 1 eq.) and 109 mg of NaH (4.54 mmol, 1.88 eq.) were dissolved in 80 ml of THF at 0°C and stirred at room temperature overnight. After filtration, all volatiles were removed under reduced pressure, and the resulting solid was washed with 10 ml of Et_2O and subsequently with 10 ml of *n*-pentane at 0°C. Drying under reduced pressure resulted in 1351 mg of **2-Na** (2.10 mmol, 87%) as a colorless solid.

^{1}H-NMR (400 MHz, THF-d_8, 25°C): δ [ppm] = 7.77 (m, 1H, 6-H), 7.12 (m, 1H, 5-H), 7.06 (m, 2H, 4-H and 3-H), 6.83 (d, 2H, $^3J_{HH}$ = 7.5 Hz, 15-H), 6.72 (t, $^3J_{HH}$ = 7.5 Hz 1H, 16-H), 6.68 (dd, $^3J_{HH}$ = 8.4 Hz, $^3J_{PH}$ = 4.8 Hz, 2H, 8-H), 6.53 (dd, $^4J_{PH}$ = 4.5 Hz, $^4J_{HH}$ = 2.3 Hz, 2H, 11-H), 6.41 (dd, $^3J_{HH}$ = 8.4 Hz, $^4J_{HH}$ = 2.3 Hz,

2H, 9-H), 3.76 (s, 6H, 20-H), 3.69 (s, 6H, 19-H), 3.52 (vhept, 2H, 17-H), and 0.92 (d, $^3J_{HH}$ = 6.8 Hz, 12H, 18-H). $^{13}C\{^1H\}$-NMR (101 MHz, THF-d_8, 25°C): δ [ppm] = 163.3 (d, $^2J_{PC}$ = 17.0 Hz, C_q, C12), 162.9 (s, C_q, C10), 154.5 (d, $^2J_{PC}$ = 24.9 Hz, C_q, C1), 146.7 (s, C_q, C14), 143.7 (s, C_q, C13), 136.6 (s, CH, C8), 135.1 (s, C3), 133.6 (d, $^1J_{PC}$ = 15.1 Hz, C_q, C2), 129.9 (d, $^2J_{PC}$ = 4.7 Hz, CH, C6), 128.5 (s, CH, C5), 128.4 (s, CH, C4), 122.8 (s, CH, C15), 122.0 (s, CH, C16), 118.7 (d, $^1J_{PC}$ = 5.3 Hz, C_q C7), 106.1 (s, CH, C9), 99.1 (d, $^3J_{PC}$ = 2.3 Hz, CH, C11), 56.2 (s, CH_3, C19), 55.4 (s, CH_3, C20), 28.6 (s, CH, C17), and 25.0 (s, CH_3, C18). $^{31}P\{^1H\}$-NMR (162 MHz, THF-d_8, 25°C): δ [ppm] = −36.17. ESI-MS(neg) [*m/z*]: for $[M\text{-}Na]^-$ = $[C_{34}H_{39}NNaO_6PS]^-$; found (calcd.): 620.22473 (620.22412).

Synthesis of compound 3 (48, 50)

Nine hundred sixty-five milligrams of ligand **2-Na** (1.35 mmol, 1 eq.) and 357 mg of [(cod)PdMeCl] (1.35 mmol, 1 eq.) were dissolved in 15 ml of DCM at room temperature. After stirring for 5 min, 5 ml of acetone was added, and the resulting suspension was stirred for 1 hour at room temperature. All volatiles were removed under reduced pressure, and the resulting solid was redissolved in 4 ml of DCM and filtered via a polytetrafluoroethylene syringe filter. After concentration under reduced pressure, addition of 15 ml of *n*-pentane and storing at −20°C resulted in precipitation of a colorless oil, which was filtered off and dried under reduced pressure, yielding 785 mg of complex **3** (0.98 mmol, 73%) as a colorless solid.

^{1}H-NMR (400 MHz, CD_2Cl_2, 25°C): δ [ppm] = 8.54 (br, 1H, 8a-H), 7.87 (ddd, $^3J_{HH}$ = 8.3 Hz, $^4J_{PH}$ = 4.6 Hz, $^4J_{HH}$ = 1.5 Hz, 1H, 6-H), 7.41-7.34 (m, 2H, 3-H and 5-H), 7.25 (tt, $^3J_{HH}$ = 7.5 Hz, $^4J_{HH}$ = $^4J_{PH}$ = 1.4 Hz, 1H, 4-H), 7.08 (d, br, $^3J_{HH}$ = 7.0 Hz, 1H, 15a-H), 7.02 (vt, $^3J_{HH}$ = 7.0 Hz, 1H, 16-H), 6.98 (m, br, 1H, 15b-H), 6.88 (dd, $^3J_{PH}$ = 12.4 Hz, $^3J_{HH}$ = 8.6 Hz, 1H, 8b-H), 6.79 (d, br, $^3J_{HH}$ = 8.6 Hz, 1H, 9a-H), 6.55 (dd, $^4J_{PH}$ = 4.7 Hz, $^4J_{HH}$ = 2.3 Hz, 1H, 11b-H), 6.46 (d, br, $^3J_{HH}$ = 8.6 Hz, 1H, 9b-H), 6.41 (t, $^4J_{PH}$ = $^4J_{HH}$ = 2.9 Hz, 1H, 11a-H), 3.97 (br, 1H, 17a-H), 3.89 (s, 3H, 19a-H), 3.84 (s, 3H, 19b-H), 3.68 (s, 3H, 20b-H), 3.46 (s, 3H, 20a-H), 3.32 (br, 1H, 17b-H), 1.98 (s, 6H, 21-H), 1.31 (d, $^3J_{HH}$ = 6.9 Hz, 3H, 18a-H), 1.24 (d, br, $^3J_{HH}$ = 6.1 Hz, 3H, 18d-H), 1.15 (d, $^3J_{HH}$ = 6.7 Hz, 3H, 18b-H), 0.80 (d, br, $^3J_{HH}$ = 6.8 Hz, 3H, 18c-H), and −0.17 (s, 3H, 21-H). $^{13}C\{^1H\}$-NMR (101 MHz, CD_2Cl_2, 25°C): δ [ppm] = 165.2 (br, C_q, C12a), 164.1 (br, C_q, C12b), 162.4 (s, C_q, C10a), 161.9 (br, C_q, C10b), 161.6 (br, C_q, C10), 151.2 (d, $^2J_{PC}$ = 14.8 Hz, C_q, C1), 144.5 (vbr, CH, C8a), 142.3 (s, br, C_q, C13 and C14), 135.9 (br, CH, C8b), 135.2 (d, $^2J_{PC}$ = 3.4 Hz, CH, C3), 129.9 (d, $^2J_{PC}$ = 2.6 Hz, CH, C5), 127.8 (s, C_q, C2), 127.5 (d, $^3J_{PC}$ = 8.3 Hz, CH, C4), 125.9 (d, $^3J_{PC}$ = 9.0 Hz, CH, C6), 124.8 (s, CH, C16), 123.8 (s, CH, C15a), 123.3 (s, CH, C15b), 105.7 (d, $^3J_{PC}$ = 16.7 Hz, CH, C9a), 105.0 (d, $^3J_{PC}$ = 10.8 Hz, CH, C9b), 99.7 (d, $^3J_{PC}$ = 6.4 Hz, CH, C11b), 98.9 (d, $^3J_{PC}$ = 5.1 Hz, CH, C11a), 56.5 (s, CH_3, C20b), 56.1 (s, CH_3, C19a), 56.0 (s, CH_3, C19b), 55.2 (s, CH_3, C20a), 31.8 (s, CH_3, C23), 28.9 (s, CH, C17a), 28.2 (s, CH, C17b), 26.3 (s, CH_3, C18c), 25.6 and 24.6 (s, CH_3, C18a and C18d), 24.2 (s, CH_3, C18b), and 2.2 (s, CH_3, C21). $^{31}P\{^1H\}$-NMR (162 MHz, CD_2Cl_2, 25°C): δ [ppm] = 26.08 (br). ESI-MS(pos) [*m/z*]: for [M-acetone + H]$^+$ = $[C_{35}H_{43}NO_6PPdS]^+$; found (calcd.): 742.15899 (742.15781). Anal. calcd. for $C_{38}H_{48}NO_7PPdS$: C, 57.03; H, 6.05; N, 1.75; S, 4.01; found: C, 54.35; H, 5.35; N, 1.68, 4.58.

Synthesis of compound 1

In a slightly opened Schlenk tube under a stream of Ar, a solution of 785 mg of compound 3 (0.98 mmol, 1 eq.) and 188 mg of 3,4-DMBA (0.98 mmol, 1 eq.) in 15 ml of DCM was stirred at room temperature for 1.5 hours. The resulting orange solution was concentrated under reduced pressure to a volume of <5 ml. Addition of 15 ml of *n*-pentane resulted in precipitation of an orange oil, which was dried under reduced pressure, resulting in 673 mg of catalyst **1** in 95% purity (0.74 mmol, 76%) as an orange solid.

^{1}H-NMR (400 MHz, CD_2Cl_2, 25°C): δ [ppm] = 8.08 (br, 1H, 8a-H), 7.87 (ddd, $^3J_{HH}$ = 7.8 Hz, $^4J_{PH}$ = 4.6 Hz, $^4J_{HH}$ = 0.7 Hz, 1H, 6-H), 7.57 (tt, $^3J_{HH}$ = 7.6 Hz, $^4J_{HH}$ = $^5J_{PH}$ = 1.7 Hz, 1H, 5-H), 7.43 (tt, $^3J_{HH}$ = 7.5 Hz, $^4J_{HH}$ = $^4J_{PH}$ = 1.6 Hz, 1H, 4-H), 7.34 (dd, $^3J_{PH}$ = 12.5 Hz, $^3J_{HH}$ = 7.7 Hz, 1H, 3-H), 7.20 (m, 2H, 16-H and 23-H), 7.08 (m, 3H, 15-H and 27-H), 6.91 (br, 1H, 8b-H), 6.72 (d, $^3J_{HH}$ = 8.3 Hz, 1H, 24-H), 6.80-6.35 (m, br, 4H, 9-H and 11-H), 3.87 (s, 6H, 20-H), 3.81 (s, 3H, 28-H), 3.72 (s, 3H, 29-H), 3.95-3.55 (br, 8H, 17-H and 19-H), and 1.33 and 1.06 (br, each 6H, 18-H). $^{13}C\{^1H\}$-NMR (101 MHz, CD_2Cl_2, 25°C): δ [ppm] = 184.3 (vbr, C_q, C21), 165.4 (br, C_q, C12), 163.1 (d, $^2J_{PC}$ = 3.6 Hz, C_q, C10), 153.5 (s, C_q, C25), 150.6 (br, C_q, C14), 149.1 (d, $^2J_{PC}$ = 12.5 Hz, C_q, C1), 148.9 (s, C_q, C26), 138.5 (s, C_q, C13), 134.4 (d, $^2J_{PC}$ = 2.4 Hz, CH, C3), 131.4 (d, $^4J_{PC}$ = 2.5 Hz, CH, C5), 129.3 (d, $^3J_{PC}$ = 9.0 Hz, CH, C4), 127.2 (s, CH, C16), 126.0 (d, $^1J_{PC}$ = 60.6 Hz, C_q, C2), 125.4 (d, $^3J_{PC}$ = 9.2 Hz, CH, C6), 125.0 (s, C_q, C22), 124.1 (s, CH, C15), 123.0 (s, CH, C23), 111.6 (s, CH, C27), 110.5 (s, CH, C24), 106.4 (d, $^3J_{PC}$ = 13.4 Hz, CH, C9), 99.6 (s, br, CH, C11), 56.5 (br, CH_3, C19 and C20), 56.3 (s, CH_3, C29), 56.1 (s, CH_3, C28), 29.4 (s, br, CH, C17), and 25.1 and 24.5 (s, br, CH_3, C18). $^{31}P\{^1H\}$-NMR (162 MHz, CD_2Cl_2, 25°C): δ [ppm] = 0.17 (br). ESI-MS(pos) [*m/z*]: for [M + Na]$^+$ = $[C_{43}H_{48}NNaO_{10}PPdS]^+$; found (calcd.): 930.16648 (930.16636). Anal. calcd. for $C_{43}H_{48}NO_{10}PPdS$: C, 56.86; H, 5.33; N, 1.54; S, 3.53; found: C, 56.10; H, 4.73; N, 1.44; S, 3.80.

Synthesis of bis-(chloro-κ^2-P,O-(bis(2-methoxyphenyl)phosphaneyl)benzenesulfonato palladium(II) (60)

To a solution of 1.21 g of 2-(*bis*(2-methoxyphenyl)phosphaneyl)-benzenesulfonic acid (3.0 mmol, 1 eq.) in 20 ml of DCM, a solution of 800 mg [(cod)PdMeCl] (3.0 mmol, 1 eq.) in 20 ml of DCM was added and stirred overnight upon which gas evolution was observed. The resulting orange solid was isolated on air using a centrifuge and washed three times with *n*-pentane. Drying under reduced pressure resulted in 1.18 g of *bis*-(chloro-κ^2-P,O-(*bis*(2-methoxyphenyl)phosphaneyl) benzenesulfonato palladium(II) (1.1 mmol, 72%), which was insoluble in all common solvents.

ESI-MS(pos) [*m/z*]: for [M + H]$^+$ = $[C_{40}H_{37}Cl_2O_{10}P_2Pd_2S_2]^+$; found (calcd.): 1084.875880 (1084.87446). Anal. calcd. for $C_{40}H_{36}Cl_2O_{10}P_2Pd_2S_2$: C, 44.22; H, 3.34; S, 5.90; found: C, 45.85; H, 3.44; S, 6.05.

Synthesis of bis-(μ$_2$-benzoato-κ^2-P,O-(bis(2-methoxyphenyl)phosphaneyl)benzenesulfonato palladium(II)

Two hundred milligrams of *bis*-(chloro-κ^2-P,O-(*bis*(2-methoxyphenyl)phosphaneyl)benzenesulfonato palladium (II) (184 μmol, 1 eq.) and 84 mg of silver benzoate (368 μmol, 2 eq.) were suspended in 6 ml of DCM and stirred for 2 hours at room temperature in the dark. A yellow solution was isolated via filtration, and all volatiles were removed under reduced pressure. Recrystallization with *n*-pentane from a DCM solution and subsequent washing with *n*-pentane resulted in 180 mg of **1b** (286 μmol, 78%) as an orange

solid. Single crystals, suitable for x-ray diffraction analysis, were obtained by slow diffusion of *n*-pentane into a solution of **1b** in DCM.

^{1}H-NMR (400 MHz, CD_2Cl_2, 25°C): δ [ppm] = 8.07 (dd, $^3J_{HH}$ = 7.8 Hz, $^4J_{HH}$ = 4.6 Hz, 2H, 6-H), 7.80 (br, 4H, 8-H), 7.61 (m, 2H, 5-H), 7.52 (t, $^3J_{HH}$ = 8.0 Hz, 4H, 10-H), 7.37 (m, 2H, 4-H), 7.33 (m, 2H, 3-H), 7.29 (vm, 2H, 17-H), 7.28 (vt, $^3J_{HH}$ = 7.4 Hz, 4H, 15-H), 7.10 (t, $^3J_{HH}$ = 7.4 Hz, 4H, 16-H), 7.01 (dd, $^3J_{HH}$ = 8.1 Hz, $^4J_{HH}$ = 5.5 Hz, 4H, 11-H), 6.83 (br, 4H, 9-H), and 3.57 (br, 12H, 18-H). ^{13}C{^{1}H}-NMR (101 MHz, CD_2Cl_2, 25°C): δ [ppm] = 177.3 (br, C13), 161.3 (d, $^2J_{PC}$ = 1.9 Hz, C12), 147.6 (d, $^2J_{PC}$ = 12.6 Hz, C1), 136.9 (br, C8), 134.9 (d, $^4J_{PC}$ = 2.1 Hz, C10), 134.7 (d, $^2J_{PC}$ = 2.8 Hz, C3), 133.8 (br, C14), 132.03 (s, C17), 132.00 (s, C5), 130.1 (s, C15), 129.5 (d, $^3J_{PC}$ = 8.7 Hz, C4), 127.8 (s, C16), 127.5 (d, $^3J_{PC}$ = 9.1 Hz, C6), 125.1 (d, $^1J_{PC}$ = 62.9 Hz, C2), 121.6 (d, $^3J_{PC}$ = 12.7 Hz, C9), 112.5 (br, C11), and 56.2 (s, C18). ^{31}P{^{1}H}-NMR (162 MHz, CD_2Cl_2, 25°C): δ [ppm] = 3.28 (br). ESI-MS(pos) [*m*/*z*]: for [M + Na]$^+$ = $[C_{54}H_{46}NaO_{14}P_2Pd_2S_2]^+$; found (calcd.): 1278.978570 (1278.976446). Anal. calcd. for $C_{54}H_{46}O_{14}P_2Pd_2S_2$: C, 51.56; H, 3.69; S, 5.10; found: C, 53.23; H, 3.94; S, 5.61. X-ray diffraction: M_w = 1342.78 g mol^{-1}; monoclinic; space group: *C*2/*c*; *a* = 17.0274(10) Å; *b* = 17.8526(10) Å; *c* = 19.3763(11) Å; α = 90°; β = 112.560(1)°; γ = 90°; *V* = 5540.41 Å3; *R* = 3.7%.

Synthesis of compound 2b-H (48)

To a solution of 10.0 g of *N*-(2,6-diisopropylphenyl)benzenesulfonamide (31.65 mmol, 1 eq.) in 160 ml of THF, 41.5 ml of *n*-BuLi (1.6 M in hexanes, 66.47 mmol, 2.1 eq.) was added dropwise at 0°C. After stirring for 2 hours at room temperature, a solution of 8.2 g of chlorobis(4-fluorphenyl)phosphane (31.65 mmol, 1 eq.) in 100 ml of THF was added dropwise at −78°C. After stirring at room temperature overnight, volatiles were removed under reduced pressure, and 200 ml of water and 150 ml of DCM were added. After acidification with 10 ml of HCl (4 N dioxane), phases were separated and the aqueous phase was extracted three times with 150 ml of DCM. The combined organic phases were dried over $MgSO_4$, and all volatiles were removed under reduced pressure. After recrystallization from 200 ml of MeOH and 25 ml of DCM, 12.54 g of **2b-H** (23.32 mmol, 74%) was yielded as a colorless solid.

^{1}H-NMR (400 MHz, 298 K, CD_2Cl_2): δ [ppm] = 7.90 (m, 1H, 6-H), 7.48 (m, 2H, 4- and 5-H), 7.29 (m, 6H, 3-, 9-and 16-H), 7.14 (m, 6H, 8-and 13-H), 3.23 (hept, $^3J_{HH}$ = 6.8 Hz, 2H, 15-H), and 1.02 (d, $^3J_{HH}$ = 6.8 Hz, 12H, 16-H). ^{13}C{^{1}H}-NMR (101 MHz, 298 K, CD_2Cl_2): δ [ppm] = 164.20 (C_q, C10), 149.51 (C_q, C12), 147.19 (C_q, C1), 146.93 (d, J_{PC} = 4.9 Hz, C_q, C7), 136.61 (Cq, C2), 136.59 (CH, C3), 136.19 (dd, $^2J_{CP}$ = 21.1 Hz, $^3J_{CF}$ = 8.1 Hz, CH, C8), 133.04 (CH, C4), 131.88 (Cq, C11), 130.24 (CH, C5), 129.45 (CH, C14), 129.36 (CH, C6), 124.52 (CH, C13), 116.48 (dd, $^2J_{CF}$ = 21.1 Hz, $^3J_{CP}$ = 8.1 Hz, CH, C9), 29.49 (CH, C15), and 24.27 (CH_3, C16). ^{31}P{^{1}H}-NMR = (120 MHz, 298 K, CD_2Cl_2): δ [ppm] = −12.79 (s). ^{19}F{^{1}H}-NMR = (280 MHz, 298 K, CD_2Cl_2): δ [ppm] = −112.33 (d, $^3J_{FH}$ = 4.5 Hz). ESI-MS(pos) [*m*/*z*]: for [M + Na]$^+$ = $[C_{30}H_{30}F_2NNaO_2PS]^+$; found (calcd.): 560.15915 (560.15951). Anal. calcd. for $C_{30}H_{30}F_2NO_2PS$: C, 67.02; H, 5.62; N, 2.61; found: C, 70.84; H, 5.72; N, 2.60.

Synthesis of ligand 2b-Na

A 12.54 g of **2b-H** (23.32 mmol, 1 eq.) and 838.5 mg of NaH (34.95 mmol, 1.5 eq.) were suspended in 250 ml of THF and stirred at room temperature overnight. After filtration over Celite, all volatiles were removed under reduced pressure. Washing with 60 ml of Et_2O resulted in 12.10 g of **2b-Na** (21.62 mmol, 92%) as a colorless solid.

^{1}H-NMR (400 MHz, 298 K, acetone-d_6): δ [ppm] = 7.72 (m, 1H, 6-H), 7.22 (m, 6H, 4-, 5-and8-H), 7.08 (m, 1H, 3-H), 7.01 (m, 4H, 9-H), 6.90 (m, 2H, 13-H), 6.84 (m, 1H, 14-H), 3.75 (hept, $^3J_{HH}$ = 6.8 Hz, 2H, 15-H), and 0.82 (d, $^3J_{HH}$ = 6.8 Hz, 12H, 16-H). ^{13}C{^{1}H}-NMR (101 MHz, 298 K, acetone-d_6): δ [ppm] = 164.87 (C_q, C10), 154.21 (Cq, C11), 146.67 (C_q, C12), 142.62 (C_q, C1), 136.44 (dd, $^2J_{CP}$ = 21.0 Hz, $^3J_{CF}$ = 8.0 Hz, CH, C8), 135.90 (CH, C3), 134.82 (Cq, C7), 134.03 (C_q, C2), 129.45 (CH, C4), 129.36 (CH, C5), 129.24 (CH, C6), 123.26 (CH, C13), 122.45 (CH, C14), 115.95 (dd, $^2J_{CF}$ = 21.0 Hz, $^3J_{CP}$ = 7.3 Hz, CH, C9), 28.40 (CH, C15), and 24.60 (CH_3, C16). ^{31}P{^{1}H}-NMR = (120 MHz, 298 K, acetone-d_6): δ [ppm] = −10.14 (s). ^{19}F{^{1}H}-NMR = (280 MHz, 298 K, acetone-d_6): δ [ppm] = −114.91 (d, $^3J_{FH}$ = 4.8 Hz). ESI-MS(neg) [*m*/*z*]: for [M-Na]$^-$ = $[C_{30}H_{29}F_2NO_2PS]^-$; found (calcd.): 536.1626 (536.1619). Anal. calcd. for $C_{30}H_{29}F_2NNaO_2PS$: C, 64.39; H, 5.22; N, 2.50; found: C, 65.43; H, 5.52; N, 1.94.

General procedure of catalytic carboxylation with catalyst 1

In a typical experiment, a stainless-steel autoclave (fig. S1) with a total volume of 20 ml, equipped with a glass inlet and a magnetic stirring bar, was charged in a glove box with 4.54 mg of catalyst **1** (5 μmol, 1 eq.) and 60 mg of LiO^tBu (0.75 mmol, 150 eq.). The autoclave was closed, transferred out of the glove box, and loaded with 6 ml of the substrate via standard Schlenk technique. It was pressurized for 20 min at room temperature with the given CO_2 pressure and stirred in a preheated aluminum cone at 750 rpm at the given temperature. After the given time, the reaction was quenched by cooling the vessel to 0°C, depressurized, and opened to the air. The reaction solution was extracted three times with 4 ml of water and once with 4 ml of 2 M aqueous NaOH. Combined aqueous phases were acidified by the addition of 3 ml of 6 N aqueous HCl and extracted three times with 25 ml of DCM. Volatiles were removed under reduced pressure, and a defined amount of 2,4,6-trimethoxybenzene was added as an external standard before NMR spectroscopic analysis. Productivity and selectivity were determined by NMR spectroscopically using 3,4-dimethoxybezene, originated from precatalyst **1**, as an internal standard. Obtained products were characterized via one-dimensional (1D)– and 2D-NMR techniques, comparison to the spectra of purchased compounds, whenever commercially available and via HRMS. For remarks on certain reactions and product characterization, see the Supplementary Materials. For tabulated values, see tables S1 and S2.

Supplementary Materials

This PDF file includes:

Supplementary Text
Figs. S1 to S16
Tables S1 to S7
References

REFERENCES AND NOTES

1. J. B. Zimmerman, P. T. Anastas, H. C. Erythropel, W. Leitner, Designing for a green chemistry future. *Science* **367**, 397–400 (2020).
2. R. Geres, A. Kohn, S. C. Lenz, F. Ausfelder, A. Bazzanella, A. Möller, Roadmap Chemie 2050: Auf dem Weg zu einer treibhausgasneutralen chemischen Industrie in Deutschland: eine

Studie von DECHEMA und FutureCamp für den VCI. (DECHEMA Gesellschaft für Chemische Technik und Biotechnologie eV, 2019).
3. J. Artz, T. E. Müller, K. Thenert, J. Kleinekorte, R. Meys, A. Sternberg, A. Bardow, W. Leitner, Sustainable conversion of carbon dioxide: An integrated review of catalysis and life cycle assessment. *Chem. Rev.* **118**, 434–504 (2018).
4. R. A. Sheldon, D. Brady, Green chemistry, biocatalysis, and the chemical industry of the future. *ChemSusChem* **15**, e202102628 (2022).
5. C. Hepburn, E. Adlen, J. Beddington, E. A. Carter, S. Fuss, N. Mac Dowell, J. C. Minx, P. Smith, C. K. Williams, The technological and economic prospects for CO2 utilization and removal. *Nature* **575**, 87–97 (2019).
6. C. Ampelli, S. Perathoner, G. Centi, CO_2 utilization: An enabling element to move to a resource- and energy-efficient chemical and fuel production. *Philos. Trans. Royal Soc.* **373**, 20140177 (2015).
7. W. Leitner, Carbon dioxide as a raw material: The synthesis of formic acid and its derivatives from CO2. *Angew. Chem. Int. Ed. Engl.* **34**, 2207–2221 (1995).
8. M. V. Solmi, M. Schmitz, W. Leitner, in *Studies in Surface Science and Catalysis* (Elsevier, 2019), vol. 178, pp. 105–124.
9. J. Hong, M. Li, J. Zhang, B. Sun, F. Mo, C–H bond carboxylation with carbon dioxide. *ChemSusChem* **12**, 6–39 (2019).
10. C.-K. Ran, L.-L. Liao, T.-Y. Gao, Y.-Y. Gui, D.-G. Yu, Recent progress and challenges in carboxylation with CO2. *Curr. Opin. Green Sustain. Chem.* **32**, 100525 (2021).
11. A. H. Liu, B. Yu, L. N. He, Catalytic conversion of carbon dioxide to carboxylic acid derivatives. *Greenh. Gases: Sci. Technol.* **5**, 17–33 (2015).
12. U. Dhawa, I. Choi, L. Ackermann, C–H carboxylations with CO_2, *in CO_2 as a Building Block in Organic Synthesis* (2020), pp. 29–57.
13. J. Luo, I. Larrosa, C–H carboxylation of aromatic compounds through CO_2 fixation. *ChemSusChem* **10**, 3317–3332 (2017).
14. A. S. Lindsey, H. Jeskey, The Kolbe-schmitt reaction. *Chem. Rev.* **57**, 583–620 (1957).
15. C. S. Yeung, V. M. Dong, Beyond Aresta's complex: Ni- and Pd-catalyzed organozinc coupling with CO_2. *J. Am. Chem. Soc.* **130**, 7826–7827 (2008).
16. K. Ukai, M. Aoki, J. Takaya, N. Iwasawa, Rhodium(I)-catalyzed carboxylation of Aryl- and alkenylboronic esters with CO_2. *J. Am. Chem. Soc.* **128**, 8706–8707 (2006).
17. J. Takaya, S. Tadami, K. Ukai, N. Iwasawa, Copper(I)-catalyzed carboxylation of Aryl- and alkenylboronic esters. *Org. Lett.* **10**, 2697–2700 (2008).
18. T. Ohishi, M. Nishiura, Z. Hou, Carboxylation of organoboronic esters catalyzed by N-heterocyclic carbene copper(I) complexes. *Angew. Chem. Int. Ed. Engl.* **47**, 5792–5795 (2008).
19. A. Correa, R. Martín, Palladium-catalyzed direct carboxylation of aryl bromides with carbon dioxide. *J. Am. Chem. Soc.* **131**, 15974–15975 (2009).
20. T. Fujihara, K. Nogi, T. Xu, J. Terao, Y. Tsuji, Nickel-catalyzed carboxylation of aryl and vinyl chlorides employing carbon dioxide. *J. Am. Chem. Soc.* **134**, 9106–9109 (2012).
21. K. Nogi, T. Fujihara, J. Terao, Y. Tsuji, Cobalt-and nickel-catalyzed carboxylation of alkenyl and sterically hindered aryl triflates utilizing CO2. *J. Org. Chem.* **80**, 11618–11623 (2015).
22. F. Rebih, M. Andreini, A. Moncomble, A. Harrison-Marchand, J. Maddaluno, M. Durandetti, Direct carboxylation of aryl tosylates by CO_2 catalyzed by in situ-generated Ni^0. *Chem. Eur. J.* **22**, 3758–3763 (2016).
23. C. Ma, C.-Q. Zhao, X.-T. Xu, Z.-M. Li, X.-Y. Wang, K. Zhang, T.-S. Mei, Nickel-catalyzed carboxylation of aryl and heteroaryl fluorosulfates using carbon dioxide. *Org. Lett.* **21**, 2464–2467 (2019).
24. A. Gevorgyan, K. H. Hopmann, A. Bayer, Formal C–H carboxylation of unactivated arenes. *Chem. Eur. J.* **26**, 6064–6069 (2020).
25. I. I. F. Boogaerts, G. C. Fortman, M. R. L. Furst, C. S. J. Cazin, S. P. Nolan, Carboxylation of N–H/C–H bonds using N-heterocyclic carbene copper(I) complexes. *Angew. Chem. Int. Ed. Engl.* **49**, 8674–8677 (2010).
26. I. I. F. Boogaerts, S. P. Nolan, Carboxylation of C–H bonds using N-heterocyclic carbene gold(I) complexes. *J. Am. Chem. Soc.* **132**, 8858–8859 (2010).
27. L. Zhang, J. Cheng, T. Ohishi, Z. Hou, Copper-catalyzed direct carboxylation of C–H bonds with carbon dioxide. *Angew. Chem. Int. Ed. Engl.* **49**, 8670–8673 (2010).
28. S. Fenner, L. Ackermann, C–H carboxylation of heteroarenes with ambient CO 2. *Green Chem.* **18**, 3804–3807 (2016).
29. O. Vechorkin, N. Hirt, X. Hu, Carbon dioxide as the C1 source for direct C–H functionalization of aromatic heterocycles. *Org. Lett.* **12**, 3567–3569 (2010).
30. A. W. Lankenau, M. W. Kanan, Polyamide monomers *via* carbonate-promoted C–H carboxylation of furfurylamine. *Chem. Sci.* **11**, 248–252 (2020).
31. A. Banerjee, G. R. Dick, T. Yoshino, M. W. Kanan, Carbon dioxide utilization via carbonate-promoted C–H carboxylation. *Nature* **531**, 215–219 (2016).
32. H. Mizuno, J. Takaya, N. Iwasawa, Rhodium(I)-catalyzed direct carboxylation of arenes with CO_2 via chelation-assisted C–H bond activation. *J. Am. Chem. Soc.* **133**, 1251–1253 (2011).
33. T. Suga, T. Saitou, J. Takaya, N. Iwasawa, Mechanistic study of the rhodium-catalyzed carboxylation of simple aromatic compounds with carbon dioxide. *Chem. Sci.* **8**, 1454–1462 (2017).
34. T. Suga, H. Mizuno, J. Takaya, N. Iwasawa, Direct carboxylation of simple arenes with CO_2 through a rhodium-catalyzed C–H bond activation. *Chem. Commun.* **50**, 14360–14363 (2014).
35. L. Song, G.-M. Cao, W.-J. Zhou, J.-H. Ye, Z. Zhang, X.-Y. Tian, J. Li, D.-G. Yu, Pd-catalyzed carbonylation of aryl C–H bonds in benzamides with CO_2. *Org. Chem. Front.* **5**, 2086–2090 (2018).
36. L. Song, L. Zhu, Z. Zhang, J.-H. Ye, S.-S. Yan, J.-L. Han, Z.-B. Yin, Y. Lan, D.-G. Yu, Catalytic lactonization of unactivated aryl C–H bonds with CO_2: Experimental and computational investigation. *Org. Lett.* **20**, 3776–3779 (2018).
37. L. Fu, S. Li, Z. Cai, Y. Ding, X.-Q. Guo, L.-P. Zhou, D. Yuan, Q.-F. Sun, G. Li, Ligand-enabled site-selectivity in a versatile rhodium(II)-catalysed aryl C–H carboxylation with CO_2. *Nat. Catal.* **1**, 469–478 (2018).
38. Y. Gao, Z. Cai, S. Li, G. Li, Rhodium (I)-catalyzed aryl C–H carboxylation of 2-arylanilines with CO2. *Org. Lett.* **21**, 3663–3669 (2019).
39. M. Börjesson, D. Janssen-Müller, B. Sahoo, Y. Duan, X. Wang, R. Martin, Remote sp^2 C–H carboxylation via catalytic 1,4-Ni migration with CO_2. *J. Am. Chem. Soc.* **142**, 16234–16239 (2020).
40. T. Saito, J. Caner, N. Toriumi, N. Iwasawa, Rhodium-catalyzed *meta*-selective C–H carboxylation reaction of 1,1-diarylethylenes via hydrorhodation-rhodium migration. *Angew. Chem. Int. Ed.* **60**, 23349–23356 (2021).
41. M. Schmalzbauer, T. D. Svejstrup, F. Fricke, P. Brandt, M. J. Johansson, G. Bergonzini, B. König, Redox-neutral photocatalytic C–H carboxylation of arenes and styrenes with CO_2. *Chem* **6**, 2658–2672 (2020).
42. P. G. Jessop, F. Joó, C.-C. Tai, Recent advances in the homogeneous hydrogenation of carbon dioxide. *Coord. Chem. Rev.* **248**, 2425–2442 (2004).
43. W.-H. Wang, Y. Himeda, J. T. Muckerman, G. F. Manbeck, E. Fujita, CO_2 hydrogenation to formate and methanol as an alternative to Photo- and electrochemical CO_2 reduction. *Chem. Rev.* **115**, 12936–12973 (2015).
44. D. Lapointe, K. Fagnou, Overview of the mechanistic work on the concerted metallation–deprotonation pathway. *Chem. Lett.* **39**, 1118–1126 (2010).
45. L. Ackermann, Carboxylate-assisted transition-metal-catalyzed C– H bond functionalizations: Mechanism and scope. *Chem. Rev.* **111**, 1315–1345 (2011).
46. A. Uhe, M. Hölscher, W. Leitner, Carboxylation of arene C–H bonds with CO_2: A DFT-based approach to catalyst design. *Chem. Eur. J.* **18**, 170–177 (2012).
47. S. Stoychev, C. Conifer, A. Uhe, M. Hoelscher, W. Leitner, A DFT study of ruthenium pincer carboxylate complexes as potential catalysts for the direct carboxylation of arenes with CO_2–meridional versus facial coordination. *Dalton Trans.* **43**, 11180–11189 (2014).
48. G. Voit, S. Jenthra, M. Hölscher, T. Weyhermüller, W. Leitner, Reversible insertion of carbon dioxide at phosphine sulfonamido Pd^{II}–aryl complexes. *Organometallics* **39**, 4465–4473 (2020).
49. M. Hölscher, G. Kemper, S. Jenthra, C. Bolm, W. Leitner, Factors governing the catalytic insertion of CO_2 into arenes–A DFT case study for Pd and Pt phosphane sulfonamido complexes. *Chem. Eur. J.* **28**, e202104375 (2022).
50. Z. Jian, L. Falivene, P. Wucher, P. Roesle, L. Caporaso, L. Cavallo, I. Göttker-Schnetmann, S. Mecking, Insights into functional-group-tolerant polymerization catalysis with phosphine–sulfonamide palladium(II) complexes. *Chem. Eur. J.* **21**, 2062–2075 (2015).
51. L. Cui, Z. Jian, A N-bridged strategy enables hemilabile phosphine–carbonyl palladium and nickel catalysts to mediate ethylene polymerization and copolymerization with polar vinyl monomers. *Polym. Chem.* **11**, 6187–6193 (2020).
52. D. Liu, Z. Xu, M. Liu, Y. Fu, Mechanistic insights into the rhodium-catalyzed aryl C–H carboxylation. *Org. Chem. Front.* **9**, 370–379 (2022).
53. M. X. Zhang, X. H. Hu, Y. H. Xu, T. P. Loh, Selective dealkylation of alkyl aryl ethers. *Asian J. Org. Chem.* **4**, 1047–1049 (2015).
54. Y. W. Lui, B. Chan, M. Y. Lui, Methylation with dimethyl carbonate/dimethyl sulfide mixtures: An integrated process without addition of acid/base and formation of residual salts. *ChemSusChem* **15**, e202102538 (2022).
55. H. Wang, M. Tucker, Y. Ji, Recent development in chemical depolymerization of lignin: A review. *J. Appl. Chem* **2013**, 1–9 (2013).
56. M. Ferrari, M. Bonaldi, Process for preparing itopride hydrochloride, U.S. Patent WO2006051079 (2006).
57. S. W. Shin, E. Jung, S. Kim, K.-E. Lee, J.-K. Youm, D. Park, Antagonist effects of veratric acid against UVB-induced cell damages. *Molecules* **18**, 5405–5419 (2013).
58. W.-S. Choi, Y.-B. Seo, P.-G. Shin, W.-Y. Kim, S. Y. Lee, Y.-J. Choi, G.-D. Kim, Veratric acid inhibits iNOS expression through the regulation of PI3K activation and histone acetylation in LPS-stimulated RAW264.7 cells. *Int. J. Mol. Med.* **35**, 202–210 (2015).

59. B. G. Schieweck, J. Klankermayer, Tailor-made molecular cobalt catalyst system for the selective transformation of carbon dioxide to dialkoxymethane ethers. *Angew. Chem. Int. Ed.* **56**, 10854–10857 (2017).
60. M. P. Conley, R. F. Jordan, *cis/trans* Isomerization of phosphinesulfonate palladium(II) complexes. *Angew. Chem. Int. Ed. Engl.* **50**, 3744–3746 (2011).
61. S. Kozuch, S. Shaik, How to conceptualize catalytic cycles? The energetic span model. *Acc. Chem. Res.* **44**, 101–110 (2011).
62. A. Uhe, S. Kozuch, S. Shaik, Automatic analysis of computed catalytic cycles. *J. Comput. Chem.* **32**, 978–985 (2011).
63. D. H. Barich, M. T. Zell, D. R. Powell, E. J. Munson, 2,4-Dimethoxybenzoic acid and 2,5-dimethoxybenzoic acid. *Acta Crystallogr. C.* **60**, o261–o262 (2004).

Acknowledgments
Funding: This study was part of our activities in the "Fuel Science Center" under Germany's Excellence Strategy–Cluster of Excellence 2186 (ID: 390919832). **Author contributions:** Conceptualization: All authors. Methodology: All authors. Investigation: G.K. Visualization: G.K. Funding acquisition: W.L. Project administration: W.L. Supervision: W.L. Writing—original draft: G.K. Writing—review and editing: All authors. **Competing interests:** The authors declare that they have no competing interests. **Data and materials availability:** All data needed to evaluate the conclusions in the paper are present in the paper and/or the Supplementary Materials.

Submitted 12 October 2022
Accepted 30 December 2022
Published 3 February 2023
10.1126/sciadv.adf2966